



Research Article

# Theoretical Study of Methane Dissociation on Pt(111) Surface Using Density Functional Theory (DFT) Calculations

Zahraa Al-Auda<sup>1</sup>, Keith L. Hohn<sup>2</sup>

<sup>1</sup>Department of Chemical Engineering, The University of Technology, Baghdad, 10066, Iraq.

<sup>2</sup>Department of Chemical, Paper, and Biomedical Engineering, Miami University, 64 Engineering Building 650 E. High St, Oxford, OH 45056, USA.

Received: 2<sup>nd</sup> August 2023; Revised: 29<sup>th</sup> September 2023; Accepted: 30<sup>th</sup> September 2023  
Available online: 2<sup>nd</sup> October 2023; Published regularly: October 2023



## Abstract

In this work, methane (CH<sub>4</sub>) dissociation on Pt(111) surface dissociation was studied based on density functional theory (DFT) calculations to evaluate the nature of adsorption and to calculate the rate constant. The most stable configurations for H and CH<sub>3</sub> were tested on the surface of Pt(111), and the results displayed that H tends to be adsorbed at the fcc site while CH<sub>3</sub> tends to be adsorbed at the top site. The energy of barrier and rate constant of reaction were calculated and found to be (2.28 eV) and (3.21007E-08 s<sup>-1</sup>) respectively. In addition, the adsorption energy for the reactant and products to investigate the nature of adsorption of the reactant and products on Pt(111) surface either physisorption or chemisorption. The results showed that the kind of adsorption of CH<sub>4</sub> adsorbed on the surface of Pt(111) at top site is physisorption, while CH<sub>3</sub> and H species adsorption on the Pt(111) surface is chemisorption.

Copyright © 2023 by Authors, Published by BCREC Group. This is an open access article under the CC BY-SA License (<https://creativecommons.org/licenses/by-sa/4.0>).

**Keywords:** Methane dissociation; Pt(111) Surface; DFT; Density Functional Theory; reforming

**How to Cite:** Z. Al- Auda, K.L. Hohn (2023). Theoretical Study of Methane Dissociation on Pt(111) Surface Using Density Functional Theory (DFT) Calculations. *Bulletin of Chemical Reaction Engineering & Catalysis*, 18(3), 499-505 (doi: 10.9767/bcrec.19788)

**Permalink/DOI:** <https://doi.org/10.9767/bcrec.19788>

## 1. Introduction

CH<sub>4</sub>, one of the most dominant natural gas components, has been widely utilized in synthesis of chemicals such as synthesis gas and alcohol [1], production of hydrogen and energy [2]. Recently, CH<sub>4</sub> dissociation on the surface of transition metal has drawn considerable attention either from theoretical [3–6] or experimental [7–9] studies. Generally, it is assumed that CH<sub>4</sub> dissociation on the transition metal surface step is the rate-limiting step for numerous of these heterogeneous reactions [10].

DFT calculations have been widely investigated for the dissociation of CH<sub>4</sub> on group VIII surfaces. The common suitable metals for dehydrogenation reactions are Cu, Pt, Pd, and Ni [11–20]. Aykan Akça [21] investigated the surface of pure Cu(111) and the role of doping with Pd on the dissociation of CH<sub>4</sub>. He studied the sequent dehydrogenation reaction of CH<sub>4</sub> on both the surface of pure Cu(111) and PdCu(111) using DFT calculations. The results displayed H atom and CH<sub>x</sub> (x = 0–4) species are adsorbed more strongly on the Cu(111) than on Pd-doped Cu(111) surface, and the surface of Pd-doped Cu(111) is higher active than the surface of Cu(111) [21]. Sudipta Roy studied a series of surface and subsurface Ni-Pt bimetallic surfaces using DFT calculations. It was found that acti-

\* Corresponding Author.  
Email: [alauda@ksu.edu](mailto:alauda@ksu.edu) (Z. Alauda);  
Telp: +9647723419901

vation energy barriers reduced when Ni was added to Pt(111), whereas addition of Pt to Ni(111) surface led to a linear increase in barrier [22]. Nave *et al.* [23] used DFT calculations to examine methane dissociation on five metal surfaces which are Pt(100), Pt(111), Pt(110)-(1×2), Ni(100) and Ni(111). For all five metals, the lower energy route for dissociation is on a top site, and the barriers are large, 0.66–1.12 eV. Also, they stated on the Pt surfaces, there is a strong preference to bond the methyl fragment on the top site, whereas on the surface of Ni it prefers to bond on the bridge or hollow sites. For the dissociation of CH<sub>4</sub> on the Pt (h k l) surface, Petersen *et al.* [24] investigated the CH<sub>4</sub> dissociation adsorption intermediates presented CH<sub>x</sub> where x is from 0 to 3, on Pt (110) p(1 × 2) using DFT calculations. They stated the top site is favorably occupied by CH<sub>3</sub>, while CH<sub>2</sub>, CH, C are at the bridge, 3-fold fcc site and 4-fold sites respectively. Zhang *et al.* [25] studied CH<sub>4</sub> dissociation on Pt(h k l) surfaces. They investigated the adsorption sites which are favorable and stable configurations of CH<sub>x</sub>, where x is from 0 to 4 and H species on the surfaces of Pt with (100), (110), and (111) orientations. Over Pt(111), they found that the most stable configuration is an adsorption on the top site. For CH<sub>3</sub>, only one stable structure can be obtained over the top site where the initial structures at the hcp, fcc, and bridge sites are chosen to be on the top site. Three stable structures for H are found which are the top, fcc and hcp sites where the initial structure is changed from the bridge site to the fcc site. Among these structures, it is found that H prefers to be adsorbed at the fcc site.

Newly, theoretical calculations have become a potent research tool for comprehension the chemical reactions either at atomic or at molecular level. Particularly, DFT calculations can predict the precise reaction barriers, energetic and geometries [26]. Few theoretical studies focused on dissociation of CH<sub>4</sub> on Pt(111) [25,27,28]. Also, for all we know, there is no researcher interested in estimating the reaction rate constant for dissociation of CH<sub>4</sub> on Pt(111) based on DFT calculations. In this work, CH<sub>4</sub> dissociation on the surface of Pt(111) was studied to estimate the rate constant based on DFT calculations. Also, the most stable configurations for H and CH<sub>3</sub> were investigated on the surface of Pt(111), various adsorption sites on Pt(111) surface can be considered to be top, bridge, fcc and hcp sites. The total energy and barrier energy of the initial, transition and final states also were calculated. In addition, the adsorption energy for the reactant and prod-

ucts were found to know the nature of adsorption of the reactant and products on Pt(111) surface: either physisorption or chemisorption.

## 2. Computational Methods and Model

DFT periodic calculations were carried out using the Vienna ab initio simulation package (VASP) [29,30]. The Perdew-Burke-Ernzerhof (PBE) generalized gradient approximation (GGA) was utilized for the correlation and exchange energy. A cutoff energy of 400 eV was employed for the plane wave basis set. The meshes of k-points were set to 4×4×1 for Pt(111) surface to model the Brillouin zone. Because Pt is a paramagnetic element, spin polarization can be neglected [25]. For optimizing the structure and the energy calculation, the convergence criteria were set to  $1 \times 10^{-6}$  eV/atom for the tolerance of SCF. Transition states (TS) was located using the climbing-image nudged elastic band (CI-NEB) method by taking 5 images to search the minimum energy path and to estimate the activation energy of the reactions where the NEB is used to provide the initial guess of the transition state. Then using the structure of that image with the highest potential energy as an input structure to specify the precise location of the transition state via dimer method.

The surface of Pt(111) was simulated via a periodic slab with four atomic layers and a full relaxation of the upper two layers and fix of the bottom two layers as shown in Figure 1. In this work, the super cell with p(2×2) was chosen in the calculation to represent the coverage of pre-adsorbed CH<sub>4</sub> atom. The vacuum space which separates the slabs in the perpendicular direction to the surface was set to 18.3 Å. The adsorption sites of Pt(111) surface are top, bridge, hcp and fcc.

The energy of adsorption is described as in Equation (1):

$$E_{\text{ads}} = E_{(\text{adsorbate/surface})} - E_{\text{surface}} - E_{\text{adsorbate}} \quad (1)$$

where,  $E_{(\text{adsorbate/surface})}$  is the total adsorbate energy on the slab model,  $E_{\text{surface}}$  is the total ener-

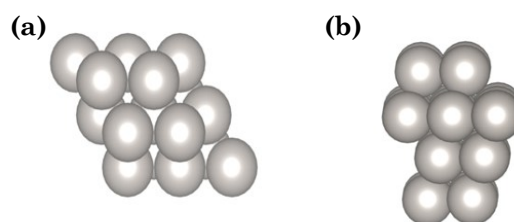


Figure 1. (a) Top and (b) side view of Pt(111) slab model.

gy of the clean surface of Pt(111), and  $E_{\text{adsorbate}}$  is the total energy of species isolated (free adsorbate).

### 3. Results and Discussion

#### 3.1 Single Adsorption of CH<sub>4</sub>, CH<sub>3</sub> and H on Pt(111) Surface

It is important to be aware of the discrete bonding natures of distinct adsorbed species on the Pt(111) surface before examining the CH<sub>4</sub>

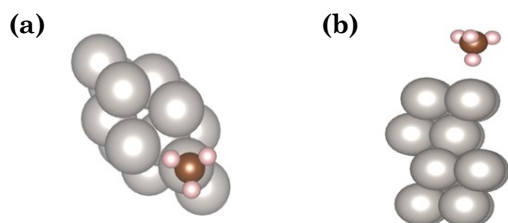


Figure 2. (a) Top view and (b) side view of CH<sub>4</sub> at top site on the surface of Pt(111).

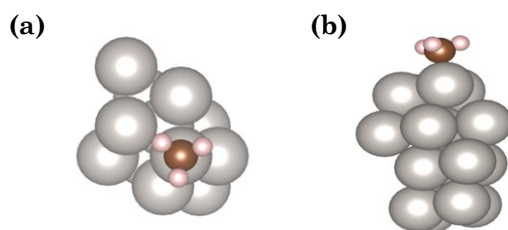


Figure 3. (a) Top view and (b) side view of CH<sub>3</sub> on surface of Pt(111).

dissociation mechanism on Pt(111) surface. Therefore, we examined the most stable configurations of CH<sub>3</sub> and H on the surface of Pt(111) to obtain the most stable structures of co-adsorbed (H-CH<sub>3</sub>) on the surface of Pt(111) as a final state.

##### 3.1.1 CH<sub>4</sub> adsorbed on Pt(111) surface

In general, the CH<sub>4</sub> adsorption on the surfaces of transition metal is categorized as a physical adsorption which emerges from the van der Waals force. The stable structures observed for initial state of CH<sub>4</sub> are at the top, bridge, hcp and fcc sites, respectively [25].

For initial state, we assume that the adsorption on the top site is the most stable configuration, building on Zhang *et al.* results [25], as displayed in Figure 2. For the CH<sub>4</sub> adsorption energy, it was found to be (13.63 kJ.mol<sup>-1</sup>) while Zhang *et al.* [25] acquired an energy of adsorption of 3.8 kJ.mol<sup>-1</sup> on the top site. Dianat *et al.* [31] evaluated an energy adsorption of 7.7 kJ.mol<sup>-1</sup> for CH<sub>4</sub> adsorption upon the surface of Pt(111) utilizing DFT slab calculations. This small magnitude confirms that the adsorption of CH<sub>4</sub> on Pt(111) is physisorption.

##### 3.1.2 CH<sub>3</sub> adsorbed on Pt(111) surface

The initial structures of CH<sub>3</sub> on the hcp, fcc, and bridge sites are selected on the top site, so one stable configuration can be acquired at the top site as can be seen from the Figure 3. The

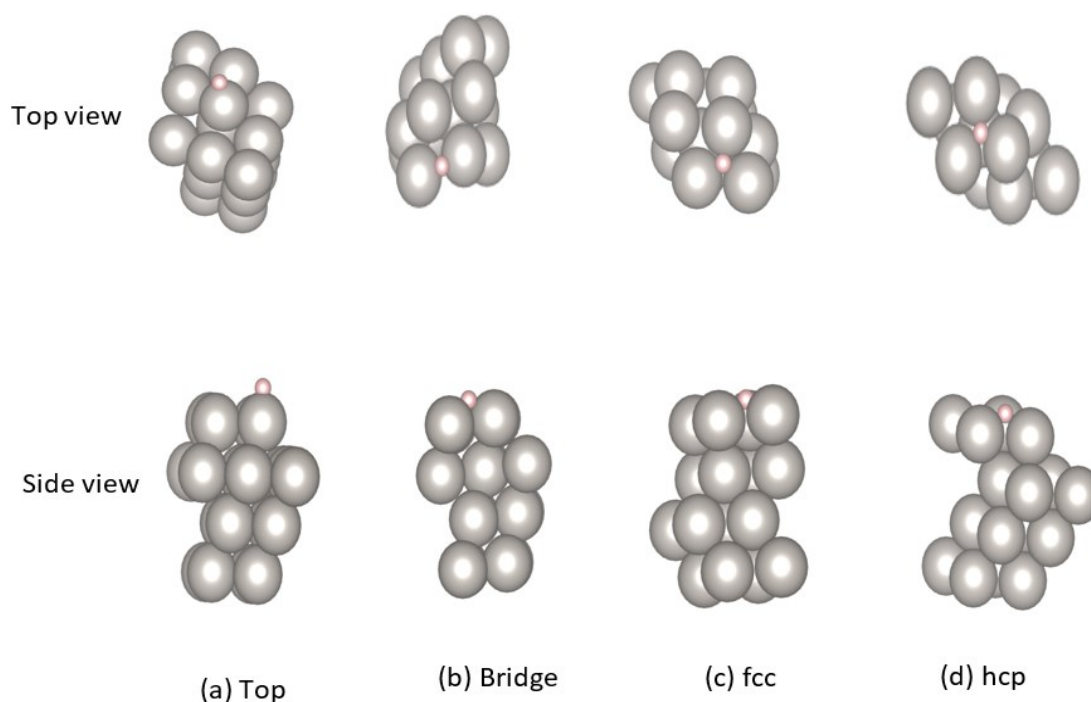


Figure 4. Top and side views of H on the surface of Pt(111) at different sites.

energy of adsorption for  $\text{CH}_3$  over the top site is  $-2.7$  eV ( $-262$  kJ.mol $^{-1}$ ). The length of C-Pt bond is  $2.077$  Å, and lengths of all C-H bonds are  $1.097$  Å which is consistent with the Zhang *et al.* [25].

### 3.1.3 H adsorbed on Pt(111) surface

For an H atom, four stable structures are found which are at the top, bridge, fcc and hcp sites as shown in Figure 4. The most stable configuration for adsorption H was found at the fcc site where the energy of adsorption is  $-3.727$  eV ( $-363.7$  kJ.mol $^{-1}$ ). The lengths of H-Pt bonds are  $1.55$ ,  $1.76$ ,  $1.87$ , and  $1.869$  Å, respectively. These results are similar to the Zhang *et al.* results [25] except they obtained three stable configurations instead of four where the initial structure is changed from the bridge site to the fcc site in their work while in our work the hydrogen exists in bridge site on Pt(111) surface as displayed in Figure 4.

### 3.2 $\text{CH}_4$ Dissociation on Pt(111) Surface

For the dissociation of  $\text{CH}_4$  step into H and  $\text{CH}_3$ , the initially adsorbed  $\text{CH}_4$  on the top site was chosen as an initial state, and the most stable co-adsorbed arrangement of  $\text{CH}_3$  (on top site) and H (on fcc site) was selected to be the final state. The transition state structure for dissociation of  $\text{CH}_4$  on Pt(111) surfaces was obtained from NEB and dimer calculations as shown in Figure 5.

In this study, the total energies of the  $\text{CH}_4$  dissociation step on the surfaces of Pt(111) and energy barriers were calculated. Figure 6 depicts the energy profile of  $\text{CH}_4$  dissociation on Pt(111) showing the energy change of the dissociation of  $\text{CH}_4$  from  $\text{CH}_4$  to  $\text{CH}_3$  and H. It can be seen from this figure that the dissociation of  $\text{CH}_4$  into  $\text{CH}_3$ -H on Pt(111) surface requires to overcome an energy barrier of  $2.28$  eV ( $220.15$  kJ.mol $^{-1}$ ), while barrier for the backward reaction is  $2.1$  eV ( $202.61$  kJ.mol $^{-1}$ ). The length bonds for C-H at transition state and C-H at the initial state were  $2.05646$  Å and  $1.0394$  Å, respectively.

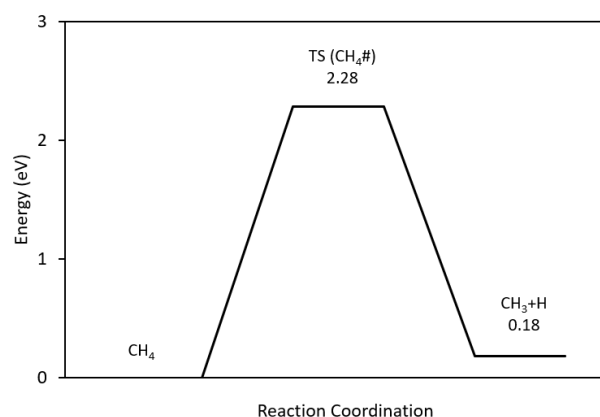


Figure 6. The energy profile scheme of  $\text{CH}_4$  dissociation to  $\text{CH}_3$  and H on the surface of Pt(111).

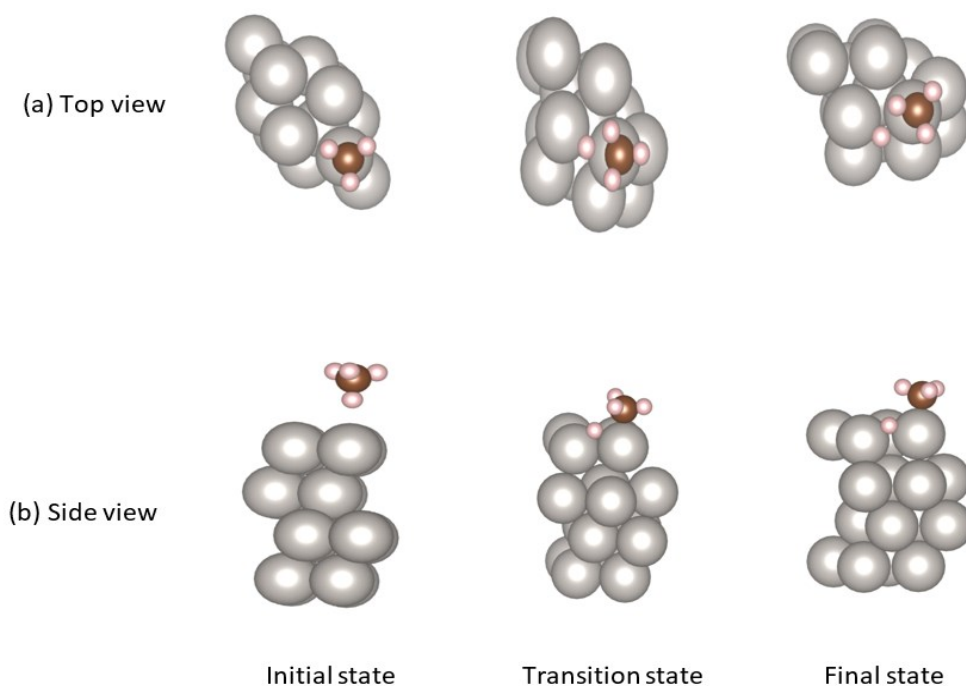
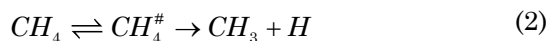


Figure 5. (a) Top view and (b) side view of  $\text{CH}_4$  dissociation on Pt(111) surface for different states.

The reaction equation of CH<sub>4</sub> dissociation can be described as in Equation (2).



To estimate the reaction rate constant, the rate constant can be calculated from Equation (3).

$$K_{TST} = \frac{K_B T}{h} \frac{q_{CH_4}^\#}{q_{CH_4}} \left( \frac{\Delta E}{RT} \right) \quad (3)$$

$$= \frac{K_B T}{h} \frac{q_{trans(3)}^\# q_{rot(3)}^\# q_{vib(8)}^\#}{q_{trans(3)} q_{rot(3)} q_{vib(9)}} \left( \frac{\Delta E}{RT} \right)$$

Table 1. CH<sub>4</sub> dissociation calculations.

<b>Initial State Calculations</b>	
For Isolated CH <sub>4</sub> (free adsorption)	$E_{\text{tot CH}_4 \text{ isolated}} = -0.23901976\text{E}+02 \text{ eV}$
For Initial state of CH <sub>4</sub> on Pt (111)	$E_{\text{tot (CH}_4 \text{ adsorbed on Pt)}} = -0.11654393\text{E}+03 \text{ eV}$ Adsorption energy = -13.63 kJ/mol
For vibrational calculations	Vibrational modes are: 3096.3 cm <sup>-1</sup> 3063.8 cm <sup>-1</sup> 2973.9 cm <sup>-1</sup> 2803.8 cm <sup>-1</sup> 1496.7 cm <sup>-1</sup> 1494.4 cm <sup>-1</sup> 1296.5 cm <sup>-1</sup> 1289.9 cm <sup>-1</sup> 1276.2 cm <sup>-1</sup>
<b>Transition State Calculations</b>	
For transition state of CH <sub>4</sub> on Pt (111)	$E_{\text{TS}} = -0.11426214\text{E}+03 \text{ eV}$
For vibrational calculations	Vibrational modes are: 3044.8 cm <sup>-1</sup> 3010.4 cm <sup>-1</sup> 2811.1 cm <sup>-1</sup> 1381.3 cm <sup>-1</sup> 1219.9 cm <sup>-1</sup> 1110.2 cm <sup>-1</sup> 958.5 cm <sup>-1</sup> 857.9 cm <sup>-1</sup> 730.6 cm <sup>-1</sup>
<b>Final State Calculations</b>	
For isolated CH <sub>3</sub> (free adsorption)	$E_{\text{tot CH}_3 \text{ isolated}} = -0.17459030\text{E}+02 \text{ eV}$
For CH <sub>3</sub> Adsorbed on Pt (111)	$E_{\text{tot (CH}_3 \text{ adsorbed at top site)}} = -0.11267099\text{E}+03 \text{ eV}$ Adsorption energy: E = -2.71 eV = -262 kJ/mol
For isolated H (free adsorption)	$E_{\text{tot H isolated}} = -0.91627852\text{E}-01 \text{ eV}$
For H adsorbed on Pt (111)	The total energies on different sites: $E_{\text{T}} = -0.96319473\text{E}+02 \text{ eV}$ $E_{\text{B}} = -0.96317967\text{E}+02 \text{ eV}$ $E_{\text{fcc}} = -0.96361804\text{E}+02 \text{ eV}$ $E_{\text{hcp}} = -0.96311756\text{E}+02 \text{ eV}$ Adsorption energies $E_{\text{T}} = -3.769\text{eV} = -359.6 \text{ kJ/mol}$ $E_{\text{B}} = -3.725 \text{ eV} = -359.4 \text{ kJ/mol}$ $E_{\text{fcc}} = -3.727 \text{ eV} = -363.7 \text{ kJ/mol}$ $E_{\text{hcp}} = -3.719 \text{ eV} = -358.8 \text{ kJ/mol}$
H-CH <sub>3</sub> co-adsorbed on Pt(111)	$E_{(\text{CH}_3\text{top-Hfcc})} = -0.11636206\text{E}+03 \text{ eV}$



where,  $K_{TST}$  is the rate constant of the reaction,  $K_B$  denotes Boltzmann's constant,  $T$  is the temperature, and  $h$  refers to Planck's constant.  $q_{trans}$ ,  $q_{rot}$ , and  $q_{vib}$  are the translational, rotational, and vibrational partition functions of  $\text{CH}_4$  over Pt(111) surface as a reactant.  $\#$  denotes transition state partition functions.  $(\Delta E)$  is the minimum energy at which reaction can occur (barrier energy). We can cancel the translational partition functions since both the transition and initial species are same. Since  $\text{CH}_4$  is a nonlinear molecule, there are 3 modes of rotational partition functions. For a nonlinear molecule, the number of vibrational modes is equal to  $3N-6$ , so there are 9 modes of vibrational partition functions for  $\text{CH}_4$  molecule. From above equation, the  $K_{TST}$  was found to be  $(3.21007\text{E}-08 \text{ s}^{-1})$ . All results are summarized in Table 1.

#### 4. Conclusion

The dissociation of  $\text{CH}_4$  on Pt(111) surface was tested using DFT calculations. From the results, one can conclude that the kind of adsorption of  $\text{CH}_4$  adsorbed at the top site of a Pt(111) surface is physisorption, while H and  $\text{CH}_3$  species adsorption on Pt(111) surface is chemisorption. On a Pt(111) surface, H tends to be adsorbed on the fcc site while  $\text{CH}_3$  tends to be adsorbed at the top site. The minimum pathway of  $\text{CH}_4$  dissociation of Pt(111) surface was achieved using Neb calculation as a first guess and then specifying the transition state location using a dimer method. Both barrier energy and reaction rate constant were calculated and found to be (2.28 eV) and  $(3.21007\text{E}-08 \text{ s}^{-1})$  respectively.

#### Acknowledgement

We would like to acknowledge Prof. Bin Liu for his suggestions.

#### CRedit Author Statement

Author Contributions: Zahraa Al-Auda: Writing, Formal analysis, Software; Keith Hohn: Review and Editing. All authors have read and agreed to the published version of the manuscript. All authors have read and agreed to the published version of the manuscript.

#### References

- [1] Hu, D., Ordonsky, V. V, Khodakov, A.Y. (2021). Major routes in the photocatalytic methane conversion into chemicals and fuels under mild conditions. *Applied Catalysis B: Environmental*, 286, 119913. DOI: 10.1016/j.apcatb.2021.119913.
- [2] Xiao, L., Wang, L. (2007). Methane activation on Pt and  $\text{Pt}_4$ : A density functional theory study. *The Journal of Physical Chemistry B*, 111(7), 1657–1663. DOI: 10.1021/jp065288e.
- [3] Abbott, H.L., Harrison, I. (2008). Methane dissociative chemisorption on Ru (0001) and comparison to metal nanocatalysts. *Journal of Catalysis*, 254(1), 27–38. DOI: 10.1016/j.jcat.2007.11.013.
- [4] Zhang, C.J., Hu, P. (2002). Methane transformation to carbon and hydrogen on Pd (100): Pathways and energetics from density functional theory calculations. *The Journal of Chemical Physics*, 116(1), 322–327. DOI: 10.1063/1.1423663.
- [5] Bunnik, B.S., Kramer, G.J. (2006). Energetics of methane dissociative adsorption on Rh {111} from DFT calculations. *Journal of Catalysis*, 242(2), 309–318. DOI: 10.1016/j.jcat.2006.06.015.
- [6] Kokalj, A., Bonini, N., Sbraccia, C., de Gironcoli, S., Baroni, S. (2004). Engineering the reactivity of metal catalysts: a model study of methane dehydrogenation on Rh (111). *Journal of the American Chemical Society*, 126(51), 16732–16733. DOI: 10.1021/ja045169h.
- [7] Huang, W., Xie, K.C., Wang, J.P., Gao, Z.H., Yin, L.H., Zhu, Q.M. (2001). Possibility of direct conversion of  $\text{CH}_4$  and  $\text{CO}_2$  to high-value products. *Journal of Catalysis*, 201(1), 100–104. DOI: 10.1006/jcat.2001.3223.
- [8] Ding, Y.H., Huang, W., Wang, Y.G. (2007). Direct synthesis of acetic acid from  $\text{CH}_4$  and  $\text{CO}_2$  by a step-wise route over Pd/SiO<sub>2</sub> and Rh/SiO<sub>2</sub> catalysts. *Fuel Processing Technology*, 88(4), 319–324. DOI: 10.1016/j.fuproc.2004.09.003.
- [9] Ukraintsev, V.A., Harrison, I. (1994). A statistical model for activated dissociative adsorption: application to methane dissociation on Pt (111). *The Journal of Chemical Physics*, 101(2), 1564–1581. DOI: 10.1063/1.468476.
- [10] Luntz, A.C., Bethune, D.S. (1989). Activation of methane dissociation on a Pt (111) surface. *The Journal of Chemical Physics*, 90(2), 1274–1280. DOI: 10.1063/1.456132.

- [11] Gao, D., Feng, Y., Yin, H., Wang, A., Jiang, T. (2013). Coupling reaction between ethanol dehydrogenation and maleic anhydride hydrogenation catalyzed by Cu/Al<sub>2</sub>O<sub>3</sub>, Cu/ZrO<sub>2</sub>, and Cu/ZnO catalysts. *Chemical Engineering Journal*, 233, 349–359. DOI: 10.1016/j.cej.2013.08.058.
- [12] Al-Auda, Z., Li, X., Hohn, K.L. (2022). Dehydrogenation of 2, 3-Butanediol to Acetoin Using Copper Catalysts. *Industrial & Engineering Chemistry Research*, 61(10), 3530–3538. DOI: 10.1021/acs.iecr.1c04181.
- [13] Saerens, S., Sabbe, M.K., Galvita, V. V., Redekop, E.A., Reyniers, M.-F., Marin, G.B. (2017). The positive role of hydrogen on the dehydrogenation of propane on Pt (111). *ACS Catalysis*, 7(11), 7495–7508. DOI: 10.1021/acscatal.7b01584.
- [14] Jiang, R., Guo, W., Li, M., Fu, D., Shan, H. (2009). Density functional investigation of methanol dehydrogenation on Pd (111). *The Journal of Physical Chemistry C*, 113(10), 4188–4197. DOI: 10.1021/jp810811b.
- [15] Al-Auda, Z., Al-Atabi, H., Li, X., Thapa, P., Hohn, K. (2019). Conversion of 5-Methyl-3-Heptanone to C<sub>8</sub> Alkenes and Alkane over Bi-functional Catalysts. *Catalysts*, 9(10), 845. DOI: 10.3390/catal9100845.
- [16] Al-Auda, Z., Al-Atabi, H., Hohn, K. (2018). Metals on ZrO<sub>2</sub>: Catalysts for the Aldol Condensation of Methyl Ethyl Ketone (MEK) to C<sub>8</sub> Ketones. *Catalysts*, 8(12), 622. DOI: 10.3390/catal8120622.
- [17] Xu, Z., Yue, Y., Bao, X., Xie, Z., Zhu, H. (2019). Propane dehydrogenation over Pt clusters localized at the Sn single-site in zeolite framework. *ACS Catalysis*, 10(1), 818–828. DOI: 10.1021/acscatal.9b03527.
- [18] Al-Auda, Z., Al-Atabi, H., Li, X., Zheng, Q., Hohn, K.L. (2019). Conversion of methyl ethyl ketone to butenes over bifunctional catalysts. *Applied Catalysis A: General*, 570, 173–182. DOI: 10.1016/j.apcata.2018.09.027.
- [19] Ma, R., Gao, J., Kou, J., Dean, D.P., Breckner, C.J., Liang, K., Zhou, B., Miller, J.T., Zou, G. (2022). Insights into the nature of selective nickel sites on Ni/Al<sub>2</sub>O<sub>3</sub> catalysts for propane dehydrogenation. *ACS Catalysis*, 12(20), 12607–12616. DOI: 10.1021/acscatal.2c03240.
- [20] Mi, C., Huang, Y., Chen, F., Wu, K., Wang, W., Yang, Y. (2021). Density functional theory study on dehydrogenation of methylcyclohexane on Ni–Pt (111). *International Journal of Hydrogen Energy*, 46(1), 875–885. DOI: 10.1016/j.ijhydene.2020.09.207.
- [21] Akça, A. (2020). CH<sub>4</sub> dissociation on the Pd/Cu (111) surface alloy: A DFT study. *Open Physics*, 18(1), 790–798. DOI: 10.1515/phys-2020-0195.
- [22] Roy, S., Hariharan, S., Tiwari, A.K. (2018). Pt–Ni subsurface alloy catalysts: an improved performance toward CH<sub>4</sub> dissociation. *The Journal of Physical Chemistry C*, 122(20), 10857–10870. DOI: 10.1021/acs.jpcc.8b01705.
- [23] Nave, S., Tiwari, A.K., Jackson, B. (2010). Methane dissociation and adsorption on Ni (111), Pt (111), Ni (100), Pt (100), and Pt (110)-(1× 2): energetic study. *The Journal of Chemical Physics*, 132(5), 54705. DOI: 10.1063/1.3297885.
- [24] Petersen, M.A., Jenkins, S.J., King, D.A. (2004). Theory of Methane Dehydrogenation on Pt {110}(1× 2). Part I: Chemisorption of CH<sub>x</sub> (x= 0– 3). *The Journal of Physical Chemistry B*, 108(19), 5909–5919. DOI: 10.1021/jp037880z.
- [25] Zhang, R., Song, L., Wang, Y. (2012). Insight into the adsorption and dissociation of CH<sub>4</sub> on Pt (h k l) surfaces: A theoretical study. *Applied Surface Science*, 258(18), 7154–7160. DOI: 10.1016/j.apsusc.2012.04.020.
- [26] Liu, H., Zhang, R., Yan, R., Wang, B., Xie, K. (2011). CH<sub>4</sub> dissociation on NiCo (1 1 1) surface: A first-principles study. *Applied Surface Science*, 257(21), 8955–8964. DOI: 10.1016/j.apsusc.2011.05.073.
- [27] Qi, Q., Wang, X., Chen, L., Li, B. (2013). Methane dissociation on Pt (1 1 1), Ir (1 1 1) and PtIr (1 1 1) surface: A density functional theory study. *Applied Surface Science*, 284, 784–791. DOI: 10.1016/j.apsusc.2013.08.008.
- [28] Ueta, H., Chen, L., Beck, R.D., Colón-Díaz, I., Jackson, B. (2013). Quantum state-resolved CH<sub>4</sub> dissociation on Pt (111): coverage dependent barrier heights from experiment and density functional theory. *Physical Chemistry Chemical Physics*, 15(47), 20526–20535. DOI: 10.1039/C3CP52244J.
- [29] Kresse, G., Furthmüller, J. (1996). Efficiency of ab-initio total energy calculations for metals and semiconductors using a plane-wave basis set. *Computational Materials Science*, 6(1), 15–50. DOI: 10.1016/0927-0256(96)00008-0.
- [30] Kresse, G., Furthmüller, J. (1996). Efficient iterative schemes for ab initio total-energy calculations using a plane-wave basis set. *Physical Review B*, 54(16), 11169. DOI: 10.1103/PhysRevB.54.11169.
- [31] Dianat, A., Seriani, N., Ciacchi, L.C., Pompe, W., Cuniberti, G., Bobeth, M. (2009). Dissociative Adsorption of Methane on Surface Oxide Structures of Pd– Pt Alloys. *The Journal of Physical Chemistry C*, 113(50), 21097–21105. DOI: 10.1021/jp905689t.